IEEE Photonics Journal
An IEEE Photonics Society Publication

Orthogonal Phase Demodulation of Optical Fiber Fabry-Perot Interferometer Based on Birefringent Crystals and Polarization Technology

Volume 12, Number 3, June 2020

Yi Huang
Shuang Wang
Junfeng Jiang
Kun Liu
Xuezhi Zhang
Peng Zhang
Tiegen Liu

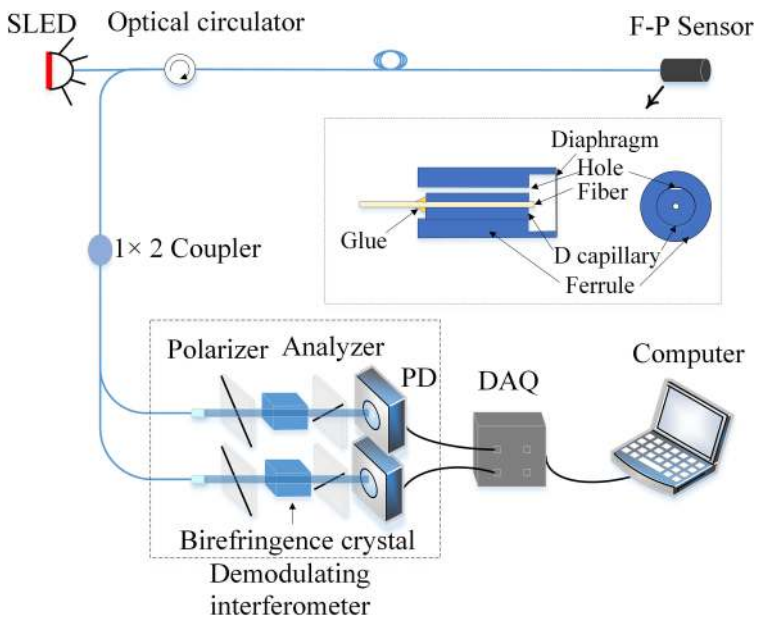

DOI: 10.1109/JPHOT.2020.2977952

Orthogonal Phase Demodulation of Optical Fiber Fabry-Perot Interferometer Based on Birefringent Crystals and Polarization Technology

Yi Huang,[1,2,3] **Shuang Wang,**[1,2,3] **Junfeng Jiang,**[1,2,3] **Kun Liu,**[1,2,3] **Xuezhi Zhang,**[1,2,3] **Peng Zhang,**[1,2,3] **and Tiegen Liu**[1,2,3]

[1]School of Precision Instrument and Opto-electronics Engineering, Tianjin University, Tianjin 300072, China
[2]Key Laboratory of Opto-electronics Information Technology, Ministry of Education, Tianjin 300072, China
[3]Tianjin Optical Fiber Sensing Engineering Center, Institute of Optical Fiber Sensing of Tianjin University, Tianjin 300072, China

DOI:10.1109/JPHOT.2020.2977952

Manuscript received July 4, 2019; revised February 24, 2020; accepted February 28, 2020. Date of publication March 6, 2020; date of current version July 14, 2020. This work was supported by National Key Research and Development Program of China under Grant 2018YFF01013203, National Natural Science Foundation of China under Grants 61735011, 61675152 and 61505139, Tianjin Natural Science Foundation under Grant 16JCQNJC02000, National Instrumentation Program of China under Grant 2013YQ030915, and China Postdoctoral Science Foundation under Grant 2016M590200. Corresponding authors: Shuang Wang; Tiegen Liu (e-mails: shuangwang@tju.edu.cn; tgliu@tju.edu.cn).

Abstract: In this paper, we propose and demonstrate the optical fiber Fabry-Perot (F-P) interferometer based on birefringent crystals and polarization technology. For recovering the variation signals, the orthogonal signals are obtained based on the birefringent crystal characteristics and the proposal thickness difference between the two crystals. The differential cross multiplication (DCM) algorithm is utilized to demodulate the orthogonal signals to obtain the phase variation of the optical fiber F-P sensor. The proposed interferometer has a minimum detection phase of 0.014 rad/$\sqrt{\text{Hz}}$ at the frequency of 25 kHz. In the experiment, two kinds of vibration signals with frequencies of 25 kHz and 15 kHz are used and the proposed interferometer SNR is 70 dB and 75 dB under the corresponding reference environment respectively. The experiment results show that the proposed interferometer can realize the measurement of large dynamic signals and has high stability. The proposed interferometer has the advantages of fast demodulation and good environmental adaptability.

Index Terms: Optical fiber Fabry-Perot interferometer, birefringent crystals, orthogonal signals, phase variation.

1. Introduction

Acoustic vibration detection is an important method for structural health monitoring [1], [2], acoustic imaging [3] and defect characterization detection [4], [5]. The optical fiber F-P sensor, which has the features of small, light, highly sensitive and anti-electromagnetic interference, is widely used in dynamic acoustic signal detection [6].

The demodulation methods for dynamic signals of optical fiber F-P sensor mainly includes intensity demodulation, wavelength demodulation and phase demodulation methods. In the intensity demodulation [7], [8] and wavelength demodulation [9] methods, the selection of linear working interval and Q point have a significant influence on the demodulation results, which restricts the working range and stability of the demodulation system. In particular, it is hard to accurately keep the sensor working in the linear interval, and the working point drifts by temperature change, static strain and other environmental perturbations. The phase demodulation methods [10], [17] can avoid the limitations of the working point and have higher sensitivity over the linear working interval. For the phase generated carrier (PGC) method [11], it has the advantages of large dynamic measurement range and high accuracy. However, the PGC method needs complicated carrier modulation, which limits the demodulation speed of high frequency signals. The white light interferometry [12] can provide absolute measurement at high resolution. However, the demodulation speed is usually limited by the complicated demodulation algorithm. Both of the PGC method and the white light interferometry are difficult to realize the demodulation of the high frequency acoustic signal.

In order to improve the demodulation speed, a dual-wavelength phase demodulation method was proposed. The dual-wavelength phase demodulation method achieved by modulating the wavelengths of two monochromatic light sources [13], [15]. The two signals with orthogonal phase differences was generated through a certain sensor cavity length in the interferometer system, and the original signal was recovered by DCM algorithm [16]. However, the two different monochromatic light sources usually have different light intensities, which increase the system instability and affect the measurement accuracy. In addition, the dual-wavelength phase demodulation method requires high accurate wavelength of the two light sources, the minor wavelength drift will affect the orthogonality of the backreflected signals and lead to error of the demodulation results. In order to avoid the influence of the different light intensities of the two light sources, the wavelength-switched phase interrogator method [17] was presented by using polarization maintaining fiber Bragg grating to generate two narrow wavelength light from broadband light source. However, the method needs to do numerous works by fitting the ellipse and eliminating the coefficients to obtain orthogonal signals for DCM algorithm. Furthermore, the accuracy of demodulation results is susceptible to fitting errors.

In this article, we proposed an interferometer based on two birefringent crystals with different thicknesses, instead of dual-wavelength monochromatic light sources, to generate the orthogonal phase and demodulate the signals by the DCM algorithm. In the system, the birefringent crystals are used to produce the optical path difference (OPD) that match the OPD formed by the optical fiber F-P sensor. According to the polarization technology and the low-coherence interference theory, only one broadband light source is needed in the system. Furthermore, the thickness of the birefringent crystals is the only factor affecting the OPD, which guarantees the stability of orthogonal phase differences. The proposed interferometer has the advantages of fast demodulation, high stability and good environmental adaptability. The proposed interferometer has a minimum detection phase of 0.014 rad/$\sqrt{\text{Hz}}$ at the frequency of 25 kHz. The experiment has demonstrated that the proposed interferometer has a large measurement range and works effectively under high frequency acoustic signals of 25 kHz and 15 kHz.

2. Principle

Fig. 1. shows the schematic of the proposed interferometer based on birefringent crystals. The optical fiber F-P sensor, consisting of fiber end face and PPS film, is used as the sensing interferometer. The broadband light in the 1550nm band emits the light through the optical circulator into the optical fiber F-P sensor, and the backreflected signal is split two channels into the demodulating interferometer via a 2 $\times$ 1 fiber coupler. The optical axis of the birefringent crystal is 45° angle with the polarization axis of the polarizer and the analyzer. The sensing interferometer and the demodulating interferometer are connected in series in the system. According to the low-coherence interference theory, when the OPD generated by the sensing interferometer and the OPD produced by the demodulating interferometer match, a significant low-coherence interference fringe signal

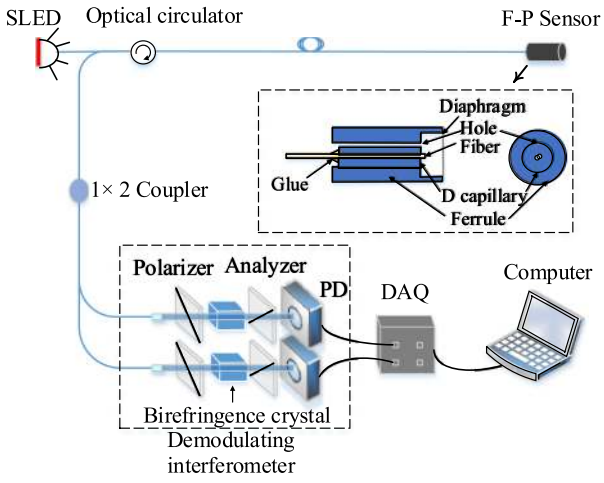

Fig. 1. Schematic of the proposed interferometer based on birefringent crystals.

appears. Then the signals are catched by the photo detector (PD, PDA50B2, THORLABS) and processed on the computer.

The F-P sensor is consisted of the sensor head(PPS film), single mode optical fiber, D borosilicate capillary and borosilicate ferrule. The F-P cavity is formed by the fiber end face and the PPS diaphragm, and the D capillary and ferrule play a supporting and fixing role, and ensure that the fiber end face and the diaphragm are parallel.

In the experiment system, the spectrum of the SLED source is Gaussian shape [18], which can be expressed as

$$S(k) = \frac{2\sqrt{\ln 2}}{\sqrt{\pi}\Delta k} \exp\left[-\frac{4\ln 2(k-k_0)^2}{\Delta k^2}\right], \tag{1}$$

where $k = 2\pi/\lambda$ is the wave number, $\Delta k = 2\pi\Delta\lambda/\lambda_0^2$, $\Delta\lambda$ is the full width at half maximum (FWHM) of the power spectrum, λ_0 and $k_0 = 2\pi/\lambda_0$ are the center wavelength and wave number of the broadband light source, respectively. The sensing interferometer can be approximated as two-beam interference, and the intensity of the low-coherence interference can be described as

$$\begin{aligned} I(d, L) &= \int_0^\infty S(k)\cos\left[k(\Delta nd - 2L)\right]dk \\ &= \exp\left[\frac{-\Delta k^2(\Delta nd - 2L)^2}{16\ln 2}\right]\cos\left[k_0(\Delta nd - 2L)\right], \end{aligned} \tag{2}$$

where Δn is the refractive index difference between extraordinary ray (E-ray) and ordinary ray (O-ray) of birefringent crystal, and d is the thickness of birefringent crystal, L is the cavity length of the optical fiber F-P sensor. Here, in order to meet the low-coherence interference condition, it is necessary to set the initial cavity length near L_0, which satisfy the condition of $\Delta nd - 2L_0 = 0$, and the cavity length varies within the coherence length.

In the interference system, by setting the difference between the thickness of the two birefringent crystals, the two signals can produce a constant $\pi/2$ phase difference. The thickness of the two birefringent crystals is d_1 and $d_2 = d_1 + \pi/2k_0\Delta n$, and the intensity of the two output signals can be expressed as

$$\begin{aligned} I_1 &= A_1 + B_1\cos\left\{k_0[\Delta nd_1 - 2L(t)]\right\} \\ I_2 &= A_2 + B_2\cos\left\{k_0[\Delta nd_2 - 2L(t)]\right\}, \end{aligned} \tag{3}$$

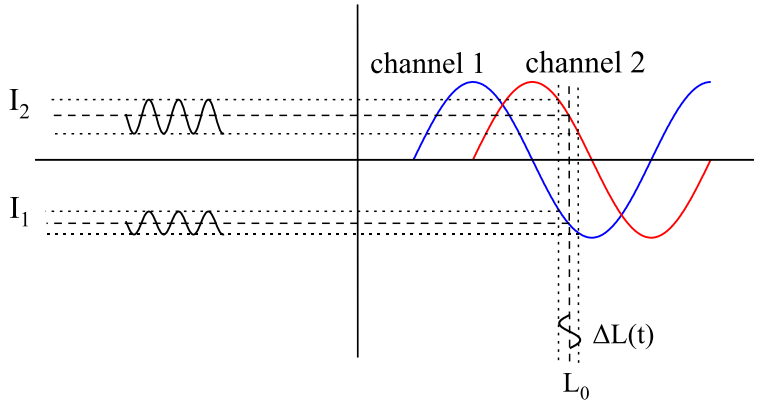

Fig. 2. Schematic of the relationship between the intensity of the working point and the static working interval.

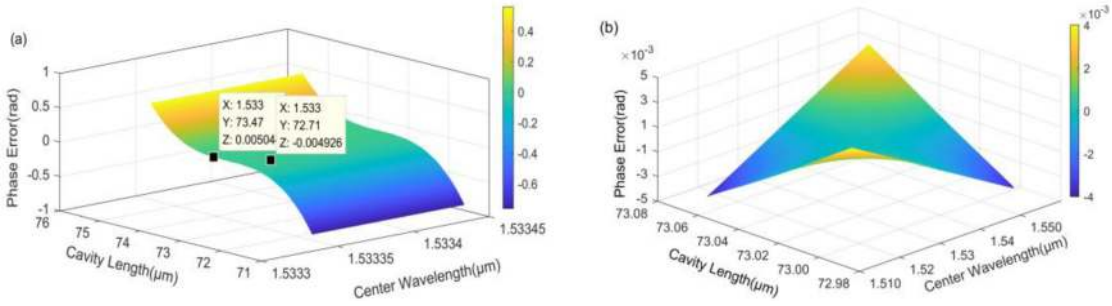

Fig. 3. Phase error simulation results of the proposed interferometer with actual thicknesses of the two birefringent crystals in the experiment system. (a) The cavity length varies in the range [71 μm, 76 μm] and the center wavelength of SLED in the range [1533.33 nm, 1533.45 nm]. (b) The center wavelength of SLED varies in the range [1510 nm, 1550 nm] and cavity length in the range [72.98 μm, 73.08 μm].

where $L(t) = L_0 + \Delta L(t)$, $\Delta L(t)$ is the change of cavity length in the time domain, A is the DC component of the interference fringe, and B is the AC component amplification coefficient. The DC component A and the AC component coefficient B can be eliminated by obtaining the static working amplitude interval, as shown in Fig. 2. We can simplify the two signals as

$$I_1 = \cos\ \varphi_t\ I_2 = \sin\varphi_t. \tag{4}$$

These two signals satisfy the condition of phase orthogonality, and the phase φ_t can be extracted by the DCM algorithm, which can be expressed as

$$\begin{aligned}\varphi_t &= \int (I_1 I_2' - I_1' I_2)dt \\ &= 2k_0 \Delta L(t),\end{aligned} \tag{5}$$

where I_1' and I_2' are the derivative of the two signals intensity respectively.

To demonstrate the proposed concept, the proposed interferometer based on birefringent crystals and polarization technology is set up. The SLED broadband light source is used with a center wavelength of 1533 nm and the FWHM is 77 nm. The material of the birefringent crystal is MgF_2. The refractive index difference between E-ray and O-ray at 1533 nm is $\Delta n \approx 0.012$. In the experiment, the distance of light beam in the crystal is changed by rotating the birefringent crystals, and the birefringent crystals have different thicknesses of d and $d + \pi/(2k_0\Delta n)$. The thickness of

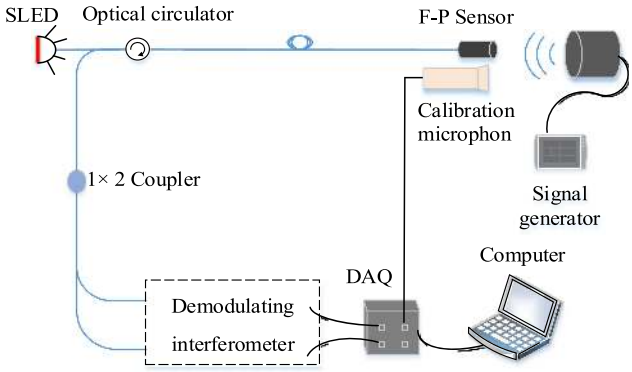

Fig. 4. Schematic of the experiment.

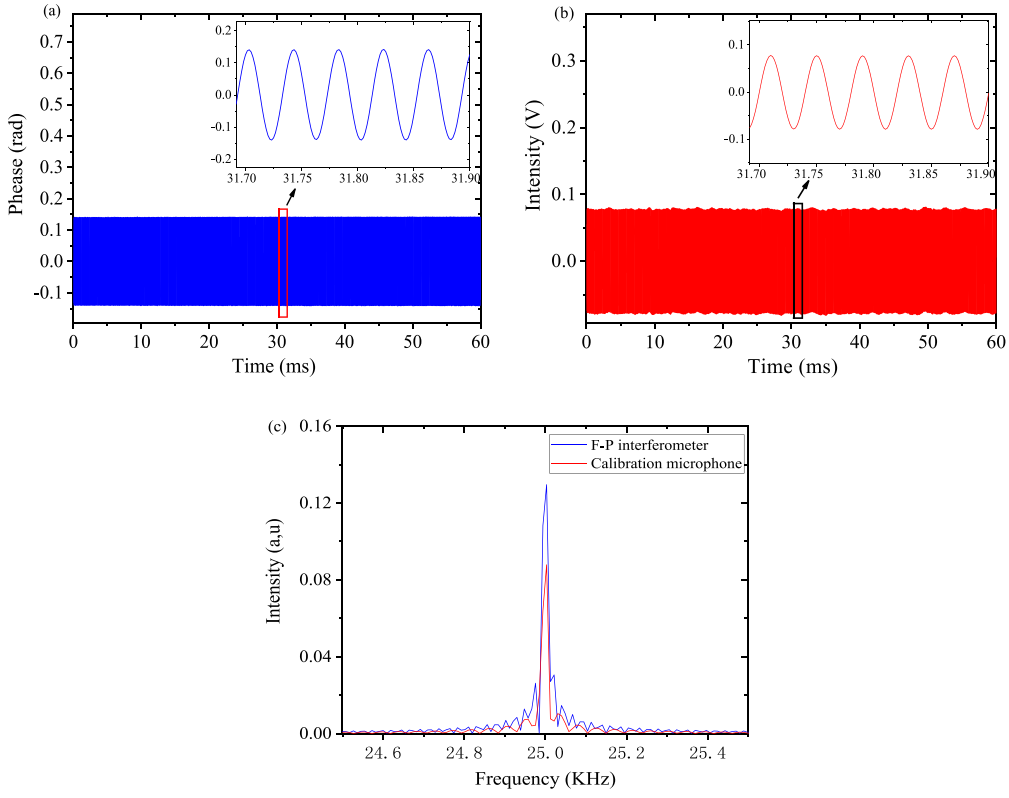

Fig. 5. Experimental results of sinusoidal sonic signals under frequency of 25 kHz with the cavity length of 73.02 μm. (a) The phase value calculated by DCM algorithm of the F-P interferometer. (b) The response signal of the calibration microphone. (c) Frequency- domain signal of the demodulated phase value and the response signal of the calibration microphone.

crystal can be obtained by using the phase trace method [19]. The optical path length of two birefringent crystals after rotation are 12.171 mm and 12.501 mm respectively. The transmission fiber type is a single mode optical fiber with a core/cladding diameter of 9/125 μm. The initial length of the optical fiber F-P cavity is 73.02 μm.

The simulation of the phase error for the demodulation results of the proposed interferometer is shown in Fig. 3. In the phase error simulation, the optical path length of the two birefringent crystals are the value of 12.171 mm and 12.501 mm in the experiment. In addition, the initial cavity length is 73.02 μm and center wavelength is 1533.38 nm. The demodulation result is subtracted from

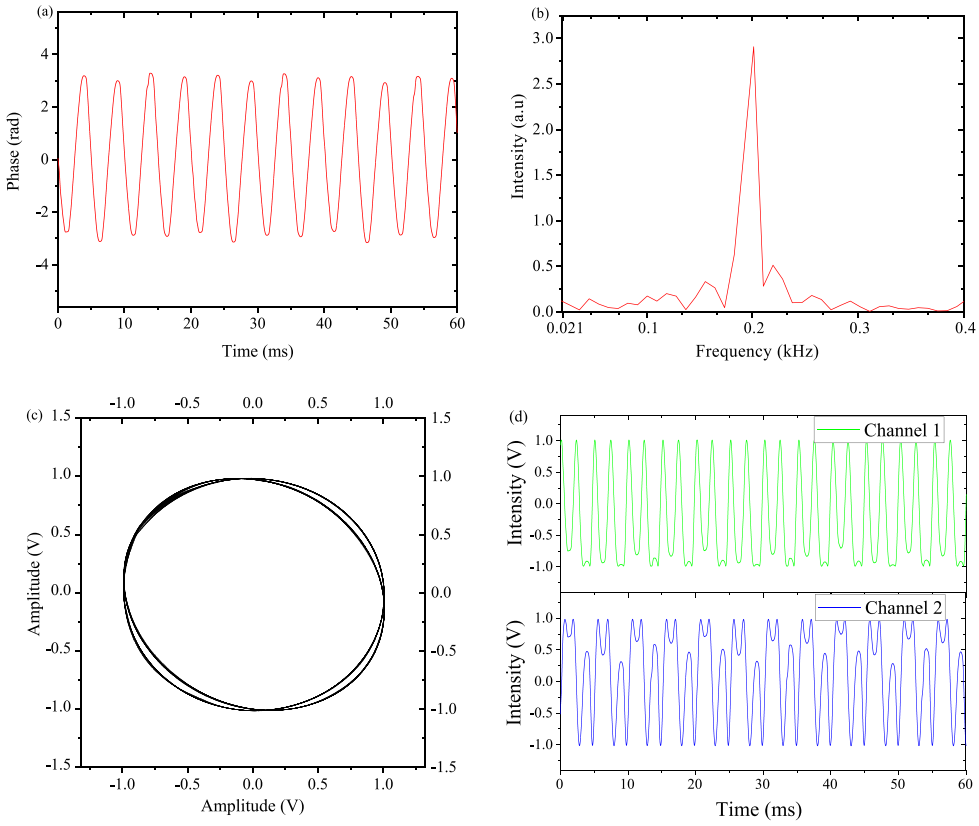

Fig. 6. Experimental results of sinusoidal signal movement at a nanopositioning stage with a frequency of 200 Hz. (a) The phase value calculated by DCM algorithm of the optical fiber F-P interferometer. (b) Frequency-domain signal of the phase value. (c) Lissajous figure. (d) The two orthogonal signals are subjected to DC processed and AC processed.

the original signal as the phase error. As shown in Fig. 3(a), the cavity length varies in the range [72.71 μm, 73.47 μm] with the center wavelength of the broadband light in the range [1533.33 nm, 1533.45 nm], and the phase error value varies in the range [-0.005 rad, $+0.005$ rad]. In the Fig. 3(b), the center wavelength of the broadband light source drifts in the rang [1510 nm, 1550 nm] with the cavity length varies in the range [72.98 μm, 73.08 μm], the phase error value varies in the range [-0.004 rad, $+0.004$ rad]. The simulation results indicate that the proposed interferometer has a small phase error under the proposed condition. According to the simulation results, the proposed interferometer has high accuracy and environmental adaptability.

3. Experimental Results and Discussion

We carried out the experiment to confirm the effectiveness of the proposed interferometer system. The schematic of the experiment is shown in Fig. 4. In the experiment, we use the signal generator to generate a sinusoidal signal which drives the PZT to arouse air vibration. The microphone (B&K, 4191) was utilized as the calibration microphone, which is placed in parallel and very close to the optical fiber F-P sensor.

The optical fiber F-P sensor cavity length is 73.02 μm. The acoustic signal generated by the PZT vibration drives the optical fiber F-P sensor's diaphragm to produce the same changes with vibration and arouse the changes in the cavity length. The PZT is driven by a sinusoidal signal of 25 kHz, and the signal received by calibration microphone is shown in Fig. 5(b). The phase

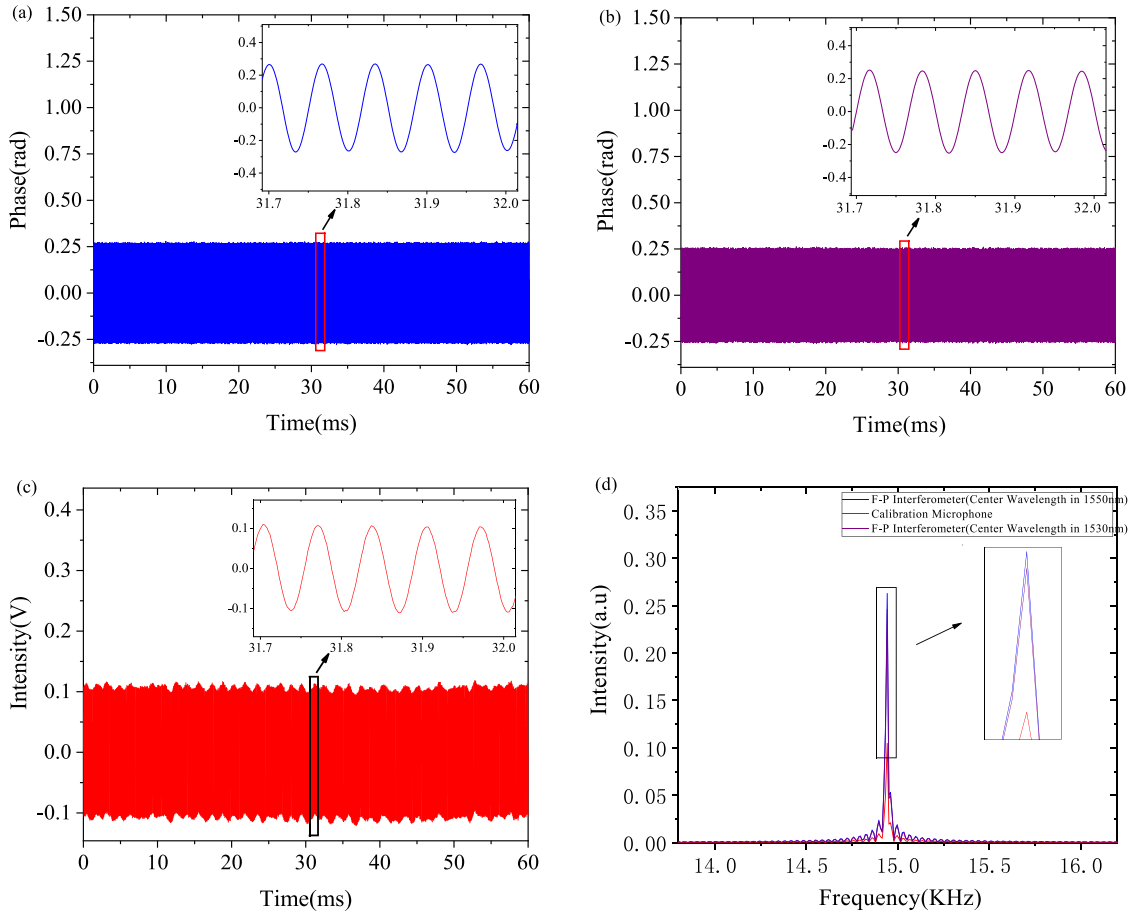

Fig. 7. Experimental results of sinusoidal sonic signals under frequency of 15 kHz with the cavity length of 72.46 μm. (a) The phase value calculated by DCM algorithm of the optical fiber F-P interferometer with the center wavelength of 1550 nm. (b) The phase value calculated by DCM algorithm of the optical fiber F-P interferometer with the center wavelength of 1530 nm. (c) The response signal of the calibration microphone. (d) Frequency-domain signal of the phase values and the response signal of the calibration microphone.

value was calculated by the DCM algorithm, shown in Fig. 5(a). The frequency-domain signal of the demodulated phase value and the response signal of the calibration microphone are shown in Fig. 5(c). The signal-to-noise ratio (SNR) of the demodulated phase value is 70 dB and the response signal of the calibration microphone SNR is 65 dB. The minimum detection phase is 0.014 rad/$\sqrt{\text{Hz}}$ of the interference system. The waveform of proposed interferometer has a great similarity to the calibration microphone and have the consistency of the frequency spectrum. The experimental results show that the proposed interferometer system can work effectively.

To confirm the ability for measuring large dynamic signals, we carried out another experiment and utilized the motion of the nanopositioning stage to change the cavity length of the optical fiber F-P sensor. The experiment results are shown in Fig. 6. In the experiment, the fiber part which forms the optical fiber F-P sensor is attached to the nanopositioning stage, and the nanopositioning stage is driven in a direction with a 200 Hz sinusoidal signal. The moving distance of the nanopositioning stage is 800 nm, satisfying the conditions that form a complete Lissajous circle. In the Fig. 6(c), it can be seen that the Lissajous figure has good orthogonality, indicating that the DCM algorithm has good applicability. The DC component and AC coefficient of two signals received by the PDs are eliminated and shown in Fig. 6(d). The phase value is calculated and shown in Fig. 6(a). The

TABLE 1
Analysis of Different Phase Demodulation Methods

Phase demodulation	Large dynamic measurement range	Fast demodulation	Good stability	Simple algorithm
phase generated carrier (PGC)	√		√	
white light interferometry	√		√	
dual-wavelength phase demodulation	√	√		√
wavelength-switched phase interrogator method	√	√	√	
orthogonal phase demodulation based on birefringent crystals and polarization technology	√	√	√	√

fast Fourier transform spectrum is shown in Fig. 6(b). The demodulation result of the proposed interferometer is very similar to the signal of the cavity length change. The frequency of the demodulation result is the same as the nanopositioning stage driving signal. It can be seen that the proposed interferometer has the ability of measure large dynamic signals.

In order to confirm the stability of the proposed interferometer under the center wavelength drift of the broadband light source, we change the center wavelength of the light source by optical fiber filter and keep the thickness of the birefringent crystals invariable. The cavity length of the optical fiber F-P sensor is 72.46 μm and the PZT is driven by a 15 kHz sinusoidal signal. The broadband light source emits the light into the interferometer system via an optical fiber filter with the center wavelength of 1550 nm and the FWHM of 15 nm. The output signals are calculated by DCM algorithm, and the phase value is shown in Fig. 7(a). We utilize another optical fiber filter to change the light signal with the center wavelength of 1530 nm and the FWHM of 15 nm, the phase value is shown in Fig. 7(b). The response signal received by calibration microphone is shown in Fig. 7(c). After the procession of fast Fourier transform, the spectrum of the demodulation results and the response of calibration microphone are shown in Fig. 7(d). The SNR of the proposed interferometer are both 75 dB.

From the experimental results, the phase values and the frequency-domain signals of the proposed interferometer have subtle differences at the center wavelengths in 1550 nm and 1530 nm. It shows that the proposed interferometer has good stability. The main reason for the difference is the mismatch of the light source and the thickness of birefringent crystals. It can be seen that after the center wavelength of the broadband light source drifted by 20 nm, the proposed interferometer can still work effectively and maintain consistency with the probed signals of calibration microphone.

4. Conclusion

This paper proposes and demonstrates an interferometer based on birefringent crystals and polarization technology. The proposed interferometer has the ability to measure large dynamic signals. The broadband light source, birefringent crystals, the polarizer and the analyzer are used to generate orthogonal signals which demodulated by the DCM algorithm. The proposed interferometer has a minimum detection phase of 0.014 rad/$\sqrt{\text{Hz}}$ at the frequency of 25 kHz. Under the acoustic signal of 15 kHz and 25 kHz, the proposed interferometer works effectively

and maintains consistency with the response signals of calibration microphone. When the center wavelengths of the light source changes from 1530 nm to 1550 nm and the thickness of birefringent crystals kept invariable, the two demodulation results of the proposed interferometer have subtle differences, which means the predominant stability of the proposed interferometer. Above all, the ability of large measurement range, the stability and the characteristic of insensitive to light source wavelength fluctuations make the proposed interferometer can be applied to many unstable environments such as pipeline monitoring in oilfield, ultrasounds detection for cracks of buildings and so on.

For comparing the proposed method of orthogonal phase demodulation based on birefringent crystals and polarization technology with other existing demodulation methods, the following table is established to obtain intuitive information.

References

[1] G. V. João, I. T. Leite, and S. Silva, TEIXEIRA, "Advanced fiber-optic acoustic sensors," *Photon. Sens.*, vol. 4, no. 3, pp. 198–208, 2014.

[2] C. Caliendo, "Latest trends in acoustic sensing," *Sensors*, vol. 14, no. 4, pp. 5781–5784, 2014.

[3] W. L. Zhang, R. Wang, and Q. Rong, "An optical fiber Fabry-Pérot interferometric sensor based on functionalized diaphragm for ultrasound detection and imaging," *IEEE Photon. J.*, vol. 9, no. 3, Jun. 2017, Art. no. 16871039.

[4] Y. Gao, M. J. Brennan, and P. F. Joseph, "On the selection of acoustic/vibration sensors for leak detection in plastic water pipes," *J. Sound Vib.*, vol. 283, no. 3, pp. 927–941, 2005.

[5] O. Hunaidi and W. T. Chu, "Acoustical characteristics of leak signals in plastic water distribution pipes," *Appl. Acoust.*, vol. 58, no. 3, pp. 235–254, 1999.

[6] B. Liu, J. Lin, and H. Liu, "Diaphragm based long cavity Fabry–Perot fiber acoustic sensor using phase generated carrier," *Opt. Common*, vol. 382, pp, 514–518, 2017.

[7] S. Wang and P. Lu, "An infrasound sensor based on extrinsic fiber-optic Fabry–Perot interferometer structure," *IEEE Photon. Technol. Lett.*, vol. 28, no. 11, pp. 1264–1267, Jun. 2016.

[8] J. Zhao, Y. Shi, and N. Shan, "Stabilized fiber-optic extrinsic Fabry–Perot sensor system for acoustic emission measurement," *Opt. Laser Technol.*, vol. 40, no. 6, pp. 874–880, 2008.

[9] Q. Wang and Z. Ma, "Feedback-stabilized interrogation technique for optical Fabry–Perot acoustic sensor using a tunable fiber laser," *Opt. Laser Technol.*, vol. 51, no. 51, pp. 43–46, 2013.

[10] K. Qian, "Two-dimensional windowed fourier transform for fringe pattern analysis: Principles, applications and implementations," *Opt. Lasers Eng.*, vol. 45, no. 2, pp. 304–317, 2007.

[11] F. Xu, J. Shi, and K. Gong, "Fiber-optic acoustic pressure sensor based on large-area nanolayer silver diaghragm," *Opt. Lett.*, vol. 39, no. 10, 2014, Art. no. 2838.

[12] C. Gouveia, M. Zibaii, and H. Latifi, "High resolution temperature independent refractive index measurement using differential white light interferometry," *Sens. Actuator B-Chem.*, vol. 188, no. 11, pp. 1212–1217, 2013.

[13] H. Liao, P. Lu, and L. Liu, "Phase demodulation of short-cavity Fabry–Perot interferometric acoustic sensors with two wavelengths," *IEEE Photon. J.*, vol. 9, no. 2, Apr. 2017, Art. no. 16795170.

[14] J.S. Jing, J. Yi, and Z. C. Liu, "Dual-wavelength DC compensation technique for the demodulation of EFPI fiber sensors," *IEEE Photon. Technol. Lett.*, vol. 30, no. 15, pp. 1380–1383, Aug. 2018.

[15] H. Wang, H. Zhao, and L. Fei, "Simultaneous phase-shifting dual-wavelength interferometry based on two-step demodulation algorithm," *Opt. Lett.*, vol. 39, no. 18, pp. 5375–8, 2014.

[16] X. Yang and Z. Chen, "A PGC demodulation based on differential-cross-multiplying (DCM) and arctangent (ATAN) algorithm with low harmonic distortion and high stability," *Proc. SPIE - The Int. Soc. Opt. Eng.*, vol. 8421, no. 2, pp. 84215J–84215J–4, 2012.

[17] J. Xia, S. Xiong, and F. Wang, "Wavelength-switched phase interrogator for extrinsic Fabry–Perot interferometric sensors," *Opt. Lett.*, vol. 41, no. 13, pp. 3082, 2016.

[18] J. Jiang, M. Xiao, S. Wang, and K. Liu, "Polarized low-coherence interferometer based on a matrix CCD and birefringence crystal with a two-dimensional angle," *Opt. Exp.*, vol. 25, no. 14, pp. 15977–15986, 2017.

[19] G. R. Pickrell, J. Xu, P. Zhang, W. Peng, H. Xiao, and A. Wang, "Novel data processing techniques for dispersive white light interferometer," *Opt. Eng.*, vol. 42, no. 11, pp. 3165–3171, 2003.